Expert Systems with Applications 39 (2012) 11149–11155

Contents lists available at SciVerse ScienceDirect

Expert Systems with Applications

journal homepage: www.elsevier.com/locate/eswa

Support Vector Machines for crop/weeds identification in maize fields

J.M. Guerrero [a,*], G. Pajares [a], M. Montalvo [b], J. Romeo [a], M. Guijarro [a]

[a] Dpto. Ingeniería del Software e Inteligencia Artificial, Facultad Informática, Universidad Complutense, Madrid 28040, Spain
[b] Dpt. Arquitectura Computadores y Automática, Facultad Informática, Universidad Complutense, Madrid 28040, Spain

ARTICLE INFO

Keywords:
Support Vector Machines
Image segmentation
Weeds/crop discrimination
Precision Agriculture

ABSTRACT

In Precision Agriculture (PA) automatic image segmentation for plant identification is an important issue to be addressed. Emerging technologies in optical imaging sensors play an important role in PA. In maize fields, site-specific treatments, with chemical products or mechanical manipulations, are applied for weeds elimination. Maize is an irrigated crop, also unprotected from rainfall. After a strong rain, soil materials (particularly clays) mixed with water impregnate the vegetative cover. The green spectral component associated to the plants is masked by the dominant red spectral component coming from soil materials. This makes methods based on the greenness identification fail under such situations. We propose a new method based on Support Vector Machines for identifying plants with green spectral components masked and unmasked. The method is also valid for post-treatment evaluation, where loss of greenness in weeds is identified with the effectiveness of the treatment and in crops with damage or masking. The performance of the method allows to verify its viability for automatic tasks in agriculture based on image processing.

1. Introduction

1.1. Problem statement

The increasing development of robotics equipped with machine vision sensors applied to Precision Agriculture (PA) is demanding solutions for several problems. The robot navigates and acts over a site-specific area of a larger farm (Davies, Casady, & Massey, 1998), where one important part of the information is supplied by the vision system.

Image segmentation is an important task related with the application of machine vision methods in PA. Efficient and automatic segmentation of vegetation from images of the ground is an important step for many applications such as weed detection for site-specific treatment (Burgos-Artizzu, Ribeiro, Tellaeche, Pajares, & Fernández-Quintanilla, 2009; Guijarro et al., 2011; Onyango & Marchant, 2003; Tellaeche, Burgos-Artizzu, Pajares, & Ribeiro, 2008a; Tellaeche, Burgos-Artizzu, Pajares, Ribeiro, & Fernández-Quintanilla, 2008b). In addition, the ground classification covers a number of ecologically relevant categories (Luscier, Thompson, Wilson, Gorham, & Dragut, 2006).

The proposed approach is intended for identifying plants (crop and weeds) in maize fields for site-specific treatments, including chemical products or mechanical manipulations, where an important goal is weeds elimination. Maize is an irrigated crop and unprotected from rainfall. After a strong rain, soil materials (particularly clays) mixed with water impregnate the vegetative cover, mainly those close or near to the soil. In this case, the green spectral component associated to the plants is masked by the dominant red spectral component coming from materials existing in the soil; Fig. 1 displays an image where this appears clearly in bottom part (center and right) of the image and also at the ends of the leaves in the maize that are oriented toward the soil. Fig. 2 displays the same occurrences at the middle left part. This makes methods based on the greenness identification, i.e. plant coverage, based on the computation of vegetation indices fail under such situations. Indeed, soil and masked plants are both identified as soil when green indices are applied. This becomes an important problem in PA because weeds densities are incorrectly identified for site specific treatments. We propose a new method based on Support Vector Machines (SVM) which makes the main contribution of this paper. The method is robust enough and works well under different lighting conditions caused by sunny or cloudy days (Tian & Slaughter, 1998). The method is valid for identifying plants with the green spectral component masked and unmasked. Moreover, the method is also valid for a post-treatment evaluation. Indeed, when weeds have been treated, they start a drying process because they are dying; this means they lost part of their greenness and the dominant spectral component becomes red instead of green, when weeds are healthy. Additionally, we can evaluate possible damage affecting crops because of the treatment assuming identical behavior with respect the red/green spectral component. Fig. 3, displays at its central inter-row crop weeds evolving toward a dry stage after the chemical treatment with herbicide, applied two days

* Corresponding author. Tel.: +34 1 3 94 75 46; fax: +34 1 3 94 75 47.
E-mail addresses: jmguerre@fdi.ucm.es (J.M. Guerrero), pajares@fdi.ucm.es (G. Pajares).

0957-4174/$ - see front matter © 2012 Elsevier Ltd. All rights reserved.
http://dx.doi.org/10.1016/j.eswa.2012.03.040

Fig. 1. Weeds in the bottom central and right part appear masked.

Fig. 2. Weeds in the middle central part appear masked.

Fig. 3. Herbicide was applied two days ago (weeds in the central inter crop rows are evolving to a dry stage). The field has received direct rainfall.

ago. This image was acquired after natural irrigation by rainfall. The proposed approach deals also well with this situation. The performance of the method allows verifying its viability for automatic tasks in agriculture based on image processing. Without loss of generality, masked plants and plants under a drying process are sometimes equally called masked in this work.

1.2. Revision of methods

Several strategies have been proposed for segmenting crop canopy images, specifically oriented towards green segmentation:

(1) Visible spectral-index based, including the excess green index (ExG, Ribeiro, Fernández-Quintanilla, Barroso, García-Alegre, 2005; Woebbecke, Meyer, von Bargen, & Mortensen, 1995), the excess red index (ExR, Meyer, Hindman, & Lakshmi, 1998), the color index of vegetation extraction (CIVE, Kataoka, 2003), the excess green minus excess red index (ExGR, Neto, 2004). The vegetative index (VEG) described in Hague, Tillet, and Wheeler (2006), which is designed to cope with the variability of natural daylight illumination. ExG, ExGR, CIVE and VEG have been applied under a combined form in Guijarro et al. (2011) gaining in performance with respect to their individual application. All these approaches need to fix a threshold for final segmentation.

(2) Specific threshold-based approaches, including dynamic thresholding. Generally, these techniques assume a two-class problem where plants and soil are to be identified. Reid and Searcy (1987) estimate a decision function under the assumption that the classes follow Gaussian distributions. The Otsu's method (Otsu, 1979) is also applied considering a bi-class problem (Ling & Ruzhitsky, 1996; Shrestha, Steward, & Birrell, 2004). These algorithms are applied to gray images. Gebhardt, Schellberg, Lock, and Kaühbauch (2006) apply also thresholding for segmentation transforming the images from RGB to gray scale intensity. This algorithm was later improved using local homogeneity and morphological operations in Gebhardt and Kaühbauch (2007). Kirk, Andersen, Thomsen, and Jørgensen (2009) apply a combination of greenness and intensity derived from the red and green spectral bands and compute an automatic threshold for a two-class problem assuming two Gaussian probability density functions associated to soil and vegetation respectively; this procedure requires the previous estimation of an angle to rotate the hypothetical greenness axis. Meyer and Camargo-Neto (2008) have applied the automatic Otsu's thresholding method for binarizing ExG and the normalized difference index (NDI), where a comparison is established against the segmentation obtained from ExGR determining that in this last case, a value of zero suffices for the threshold, therefore the Otsu's method is not required. Guijarro et al. (2011) and Burgos-Artizzu, Ribeiro, Guijarro, and Pajares (2011) have applied the statistical mean value of the transformed image obtained with the vegetation indices instead of automatic thresholding such as Otsu. They justify its choice because Otsu's method gives a threshold value higher than the mean and produces infra-segmentation.

(3) Learning-based, Meyer, Camargo-Neto, Jones, and Hindman (2004) have applied unsupervised approaches, including fuzzy clustering, for segmenting regions of interest from ExR and ExG. Tian and Slaughter (1998) proposed the environmentally adaptive segmentation algorithm (EASA) for detecting plants through a supervised learning process. Ruiz-Ruiz, Gómez-Gil, and Navas-Gracia (2009) applied the EASA later under the HSI (hue-saturation-intensity) color space to deal with the illumination variability. Zheng, Zhang, and y Wang (2009) and Zheng, Shi, and Zhang (2010) use a supervised mean-shift algorithm under the assumption that the segmentation of green vegetation from a background can be treated as a two-class segmentation problem; the class separability is validated through a neural network and the Fisher linear discriminant respectively, the color spaces used were RGB, LUV and HSI.

1.3. Motivational research of the proposed strategy

All methods above are focused on greenness identification under the assumption that the green spectral component prevails over the red one. In our problem this is not always the case, justifying the proposed strategy. Based on the considerations above concerning the different methods, the proposed strategy tries to identify plants with the green spectral component masked and unmasked. Two main stages are proposed. Firstly we apply the Otsu's thresholding approach and in the second one SVM is the chosen strategy. As reported in Meyer and Camargo-Neto (2008) the advantage of using color indices is that they accentuate a particular color, which is of interest. The images analyzed contain two main dominant spectral signatures, green for plants and red for soil. We might think to use greenness indices for the first and redness for soil identification. With such purpose, inspired on Guijarro et al. (2011) we have applied a combined strategy because of its performance as compared against individual indices but modified as follows. In Guijarro et al. (2011) ExG, ExGR, CIVE and VEG are the four indices combined. In the images analyzed in this work, ExGR causes that shadows generated by the maize plants are erroneously identified as green plants, this is an undesired effect in image segmentation because the computation of weeds pressure is affected. Therefore, ExGR is excluded from the combination. NDI is also discarded because many pixels belonging to the soil are classified as green ones. On the other hand, as reported in Guijarro et al. (2011) and Burgos-Artizzu et al. (2011), the automatic thresholding based on Otsu's method tends to produce infra-segmentation, this means that only those pixels that do not offer any doubt about its belonging to plants (weeds or crop) are identified as such. This is exactly the situation offered by unmasked plants, which are to be identified at the first stage. Therefore, we are sure that pixels classified based on Otsu belong to green plants, i.e. unmasked. At the second stage we apply SVMs on those pixels that have not been identified as unmasked plants, i.e. pixels belonging to masked plants, soil and other materials. Masked plants are finally detected by identifying support vectors. Fortunately, these support vectors, as explained later in Section 3, identify pixels belonging to masked plants or plants that have begun a drying process. Because of the learning nature derived from SVM, our strategy requires two phases: learning and decision.

In short, the design of an appropriate procedure, described in Section 2.2, allows us to identify masked and unmasked plants, minimizing the effect of shadows produced by some plants of maize.

1.4. Paper organization

This paper is organized as follows. In Section 2 we give details about the proposed strategy distinguishing clearly between learning and decision. In Section 3 the performance of the proposed strategy is proposed. Finally, in Section 4, the most relevant conclusions are extracted.

2. Strategy for plant identification

2.1. Learning phase based on Support Vector Machines

The learning phase consists of different processes outlined in the graphic displayed in Fig. 4. According to the scheme there are three main procedures: (a) Greenness identification followed by thresholding through Otsu's method to obtain a binary image, which determines two classes; (b) Identification of support vectors associated to each class, based on SVM; (c) Computation of average values for each set of support vectors, which establish limits for class separation between masked and unmasked plants.

Greenness identification and binarization: given an original input image in the RGB color space, we apply the following normalization scheme, which is usually applied in agronomic image segmentation (Gée, Bossu, Jones, & Truchetet, 2008),

$$r = \frac{R_n}{R_n + G_n + B_n}, \quad g = \frac{G_n}{R_n + G_n + B_n}, \quad b = \frac{B_n}{R_n + G_n + B_n} \tag{1}$$

where R, G and B are the normalized RGB coordinates ranging from 0 to 1 and are obtained as follows:

$$R_n = \frac{R}{R_{\max}}, \quad G_n = \frac{G}{G_{\max}}, \quad B_n = \frac{B}{B_{\max}} \tag{2}$$

where $R_{\max} = G_{\max} = B_{\max} = 255$ for our 24-bit color images.

Vegetation indices to be combined are computed as follows (see references above in Section 1.2),

$$\textit{Excess green}: \quad ExG = 2g - r - b \tag{3}$$

$$\textit{Color index of vegetation extraction}$$
$$CIVE = 0.441r - 0.811g + 0.385b + 18.78745 \tag{4}$$

$$\textit{Vegetative} \quad VEG = \frac{g}{r^a b^{1-a}}, \quad \text{with } a \text{ set to } 0.667 \text{as in Hague etal. } (2006) \tag{5}$$

Based on Guijarro et al. (2011) the above three indices are combined to obtain the resulting value COM as follows,

$$\textit{Combined}: \quad COM = w_{ExG}ExG + w_{CIVE}CIVE + w_{VEG}VEG \tag{6}$$

where w_{ExG}, w_{CIVE} and w_{VEG} are weights for each index, representing the relative importance of each index. Guijarro et al. (2011) provide the values for the four weights participating in the combination, because in this work we have excluded the *ExGR* index, the weighting values for the three indices combined are proportionally obtained, i.e. $w_{G_{ExG}} = 0.36$, $w_{G_{CIVE}} = 0.47$ and $w_{G_{VEG}} = 0.17$.

The resulting combined image COM, is linearly mapped to range in $[0,1]$, after which, it is thresholded by applying the Otsu's method, obtaining a binary image, where white pixels identify plants in the original image, with clear spectral RGB components associated to unmasked plants. On the contrary, black pixels identify those pixels in the original image belonging to masked plants, soil and other materials present in the field.

Identification of support vectors: based on the binary image, we build a partition with two classes. Class 1 (C_1) contains those pixels coming from the original image which have been labeled as white pixels in the binary image. For any white pixel located at a known spatial position in the binary image, we obtain three spectral component values from the original image, i.e. $x = (R, G, B) \in C_1$. Similarly Class 2 (C_2) contains pixels labeled as black in the binary image. Therefore, C_1 and C_2 can be considered as two subsets containing tri-dimensional patterns belonging to two different classes. The number of total patterns is n, i.e. $n = \text{card}(C_1) + \text{card}(C_2)$. The output of the SVM system is $y \in \{+1, -1\}$, where +1 and -1 are associated to classes C_1 and C_2 respectively. The training set is built as $(\boldsymbol{x}_k, y_k)$, $k = 1, \ldots, n$; where each $\boldsymbol{x}_k$ belongs either to class C_1 or C_2 and y_k denotes the label it belongs to. The goal of the training process based on SVM is to find a decision function separating tridimensional data into both classes. As displayed in Fig. 6, pattern samples $\boldsymbol{x}_k$, mapped over the 3-dimensional space appear overlapped.

Mapping input vectors into a high dimensional space through non-linear transformation functions, SVM has the ability of finding the decision function even with overlapped data (Cherkassky & Mulier, 1998; Vapnik, 2000). The SVM decision function has the following general form,

$$f(x) = \sum_{k=1}^{n} \alpha_k y_k H(x_k, x) - b \tag{7}$$

where $\boldsymbol{x}$ is a generic tri-dimensional vector whose components are the three spectral R, G, B values in the original image; b is a bias constant value to be determined. Eq. (7) defines a decision function

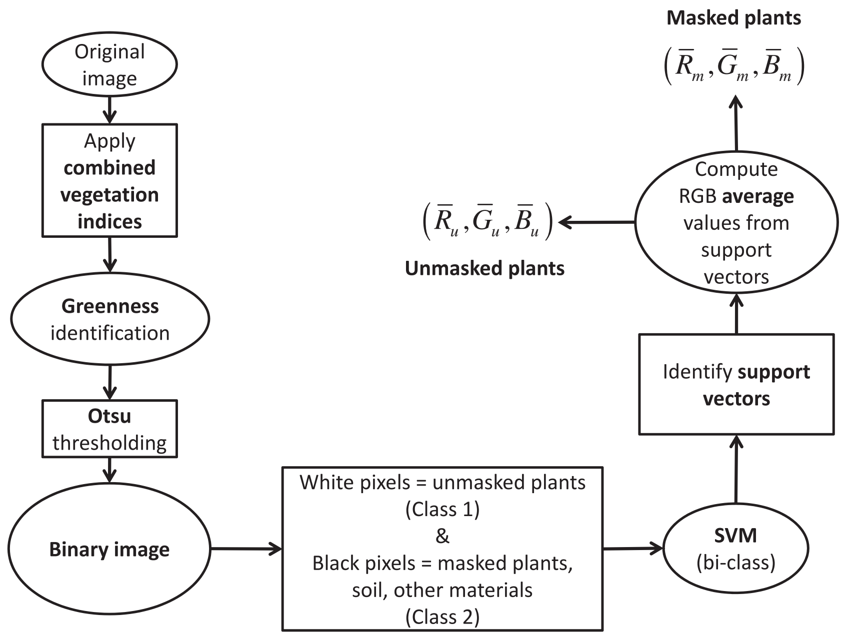

Fig. 4. Scheme of the learning procedure.

$f(\boldsymbol{x})$ as a linear combination of kernels H, centered at each data point. A discussion about the choice of the kernel used in the proposed approach is given in Section 3. Parameters α_k, $k = 1,\ldots,n$, in (7) are the solution for the following quadratic optimization problem:

$$Q(\alpha) = \alpha_k - \frac{1}{2}\sum_{k,h=1}^{n} \alpha_k \alpha_h y_k y_h H(x_k, x_h) \tag{8}$$

Subject to the following constraints,

$$\sum_{k=1}^{n} \alpha_k y_k = 0 \text{ and } 0 \le \alpha_k \le \frac{C}{2}, k = 1,\ldots,n \tag{9}$$

where H is the inner product kernel introduced above and C is a regularization parameter. In Cherkassky and Mulier (1998) is reported that there is not well-developed theory on how to select the best C, in several applications, involving SVMs, is set to a large fixed constant value, such as 2000, which is the one used in this work. Data patterns $\boldsymbol{x}_k$ associated to with the nonzero α_k are called *support vectors*, renamed as s_k, which are the main objective of this work, instead of the decision function as it is usual, in general. Support vectors are the most informative data points. The minimal distance to the separating hyperplane from the data point is the margin τ (Cherkassky & Mulier, 1998). A separating hyperplane is optimal if the margin is maximum. The distance between the separating hyperplane and a given pattern $\boldsymbol{x}_k$ is $y_k|f(x_k)|/\|w\|$ where $\boldsymbol{w}$ is a perpendicular vector to the hyperplane, given by,

$$w = \sum_{k=1}^{n} \alpha_k y_k x_k \tag{10}$$

The problem of finding the optimal hyperplane is that of finding the $\boldsymbol{w}$ that maximizes τ. Because there are infinite number of solutions that differ only in scaling of $\boldsymbol{w}$. To limit solutions, fix the scale on the product of τ and the norm $\boldsymbol{w}$,

$$\tau = \frac{1}{\|w\|} \tag{11}$$

where $\|\cdot\|$ is a norm, we have chosen the euclidean in our experiments. The bias parameter b introduced in Eq. (7) is computed as follows,

$$b = -\frac{1}{s}\sum_{k=1}^{s}(ws_k - y_k) \tag{12}$$

where $\boldsymbol{s}_k$ are the s support vectors, i.e. the s data patterns associated to with the nonzero α_k, y_k is the label initially assigned to the corresponding pattern.

Characterization of the classes: once all support vectors are obtained, we have available two sets of support vectors, S_1 and S_2, associated to classes C_1 and C_2 respectively, where $S_1 \equiv \{s_k^1\}$ with $k = 1,\ldots n_1$ and $S_2 \equiv \{s_k^2\}$ with $k = 1,\ldots n_2$; n_1 and n_2 represent the number of support vectors belonging to each class. It is well known, under the SVM framework, that support vectors represent the most significant patterns in the class they belong to. Also that they fall just in the margin of separation between classes, i.e. close to the hyperplane. Support vectors in S_1 are close to patterns in class C_2 and vice-versa. This means that support vectors establish limits between classes. So, support vectors in S_2 are exactly the closest patterns to class C_1. Because class C_1 represents plants with a degree of greenness, support vectors in S_2 are those patterns with the highest degree of greenness in class C_2. A priori they were assigned to a class different to the one containing green plants, but now they are identified as patterns with a certain degree of greenness because of their similarity to patterns in class C_1, under this assumption support vectors in class C_2 are identified as masked plants or plants affected by the treatment, which have started the dying process. We can characterize all support vectors in S_2 by computing two statistical measures, mean $\bar{x}_m = (\bar{R}_m, \bar{G}_m, \bar{B}_m)$ and standard deviation $\sigma_m = (\sigma_{mR}, \sigma_{mG}, \sigma_{mB})$. Similarly for support vectors in C_1, mean $\bar{x}_u = (\bar{R}_u, \bar{G}_u, \bar{B}_u)$ and standard deviation $\sigma_u = (\sigma_{uR}, \sigma_{uG}, \sigma_{uB})$ where sub-indices m and u denote masked and unmasked plants respectively. Means and standard deviations are the parameters obtained during the learning phase, Fig. 4.

2.2. Decision phase

Once both classes are characterized by their corresponding mean and standard deviations, they are used for a decision making process.

Given a new image containing masked and unmasked plants, the goal is to identify pixels belonging to each kind of plants.

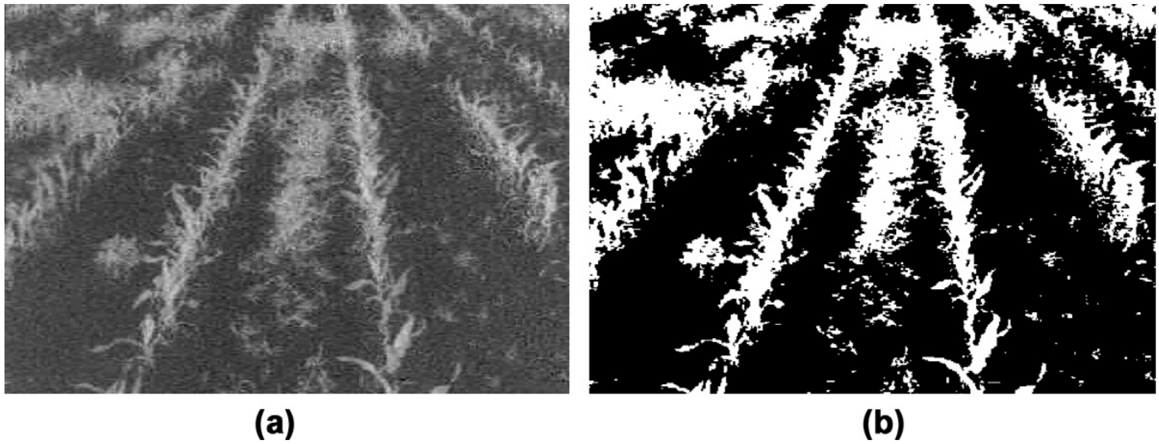

Fig. 5. Resulting images obtained from image in Fig. 1. (a) Vegetation index with the combined (COM) strategy; (b) Binary image containing masked and unmasked plants.

Because plants are characterized by the green spectral component, we compute the percentage of green from $\bar{x}_m$ and $\bar{x}_u$ as follows,

$$r_{mG} = \bar{G}_m/(\bar{R}_m + \bar{G}_m + \bar{B}_m) \quad \text{and} \quad r_{uG} = \bar{G}_u/(\bar{R}_u + \bar{G}_u + \bar{B}_u) \tag{13}$$

Also the relative deviation with respect the green spectral components,

$$t_{mG} = \sigma_{mG}/\bar{G}_m \quad \text{and} \quad t_{uG} = \sigma_{uG}/\bar{G}_u \tag{14}$$

Finally, given a pixel with its corresponding spectral components, $\boldsymbol{x} = (R,G,B)$, coming from the new image, the decision rules are established as follows,

$$\begin{aligned} &\text{Rule}(1): \quad x \in C_2 \quad \textit{if} \quad r_{mG} - t_{mG} \le G/(R+G+B) \le r_{uG} - t_{uG} \\ &\text{Rule}(2): \quad x \in C_1 \quad \textit{if} \quad r_{uG} - t_{uG} < G/(R+G+B) \end{aligned} \tag{15}$$

These rules establish limits of greenness. Rule (1) defines a region of greenness between support vectors S_1 and S_2 which allows identifying pixels belonging to masked plants or plants affected by the treatment. Rule (2) defines a region with high green spectral values, i.e. unmasked plants.

3. Results

The images used for this study were acquired with a HPR817 digital in four different days in April/May 2007. All acquisitions were spaced by five/six days. A set of them were obtained in a pre-treatment phase after the field was watered artificially and when the field received different amounts of rainfall, Figs. 1 and 2 are two representative images of this set. A second set of images were acquired in a post-treatment phase after applying a doses of herbicide, where weeds have started its decease process. Fig. 3 is a representative image of this set. Due to the difference of days in the capture, they were also acquired under different illumination conditions. This circumstance does not affect the performance of the proposed process and therefore it is not required any further study with regard to lighting.

These digital images were captured under perspective projection containing only soil and plants, i.e. without panoramic sky. They were stored as 24-bit color images with resolutions of 800×600 pixels, and saved in RGB (Red, Green and Blue) color space. The images were processed with the Image Processing Toolbox from Matlab R2009*a* (TheMathWorks, 2012). A set of 210 images were processed.

The proposed strategy is focused on the extraction of pixels belonging to unmasked and masked plants or pixels affected by the treatment. It is based on the learning phase described in Section 2.1. From the above set of available images 70 were used for identifying support vectors, which is the training set.

With respect the choice of kernel H in Eqs. (7) and (8), we have randomly selected five images from the set of 70 images used for learning. We have manually selected 1000 pixels, 500 labeled with $y_k = +1$ (class C_1) and 500 labeled with $y_k = -1$ (class C_2). Then, we randomly select the 80% of pixels from each set of 500, which are used as training patterns, from which we obtain the decision function in (7) and the parameter b in (12). The remainder 20% of selected patterns is used for validation. So, given a pattern $\boldsymbol{x}$ it is assigned to class C_1 if $f(\boldsymbol{x}) > 0$ or to class C_2 if $f(\boldsymbol{x}) \leqslant 0$. The following three kernels have been analyzed:

(1) *Gaussian Radial Basis Functions* $H(x,y) = \exp\{-\|x-y\|/\sigma^2\}$, we vary σ^2 from 1 to 10 in steps of 0.5 and for each σ^2 we compute the percentage of success obtained with the valida-

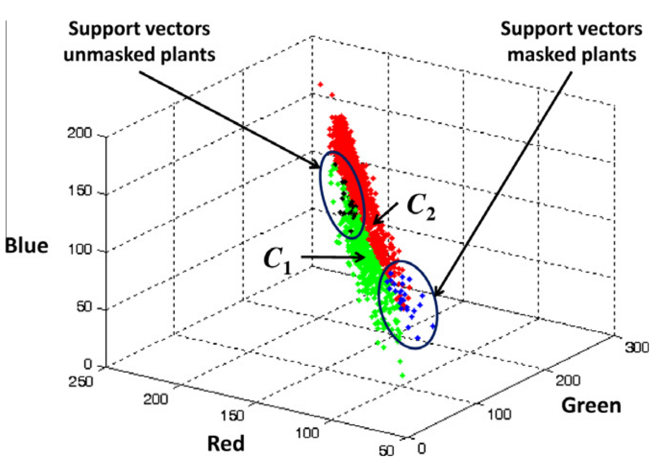

Fig. 6. Distribution of patterns and support vectors in the tridimensional RGB space.

Table 1
Number of patterns processed, support vectors obtained and parameters obtained based on the SVM framework.

Number of patterns processed	Number of support vectors	$\boldsymbol{w}$	τ	b
$800 \times 600 \times 70$	7420	$(3.3, 3.4, 2.5) \times 10^4$	1.86×10^{-5}	-1.2×10^2

Table 2
Parameters values for decision making during plant identification.

C_1				C_2			
$\bar{x}_u = (\bar{R}_u, \bar{G}_u, \bar{B}_u)$	σ_u	r_{uG}	t_{uG}	$\bar{x}_m = (\bar{R}_m, \bar{G}_m, \bar{B}_m)$	σ_m	r_{mG}	t_{mG}
(160.5, 165.5, 108.7)	(18.1, 16.3, 20.2)	0.3809	0.0984	(102.2, 100.8, 84.4)	(9.3, 10.3, 9.5)	0.3507	0.1022

tion data patterns. This process is repeated 10 times. Finally, we obtain $\sigma^2 = 3.5$ with an averaged percentage of successes of 84.2%.

(2) *Polynomial* $H(x,y) = \langle x,y \rangle^d$ with $\langle x,y \rangle$ defined as the inner product. Following the same procedure as above, but varying the parameter d from 1 to 5 in steps of 0.5, we obtain $d = 2.5$ with 79.1% of successes.

(3) *Sigmoid* $H(x,y) = \tanh(\rho\langle x,y \rangle + \gamma)$, as before, we vary ρ from 1 to 10 in steps of 0.5 and γ from 1 to 5 in steps of 0.5 obtaining $\rho = 2.5$ and $\gamma = 3.0$ with 74% of successes.

Finally, we choose Gaussian Radial Basis function because its best performance with $\sigma^2 = 3.5$.

Each binary image is obtained through the combined strategy, COM, from three vegetation indices followed by the Otsu's thresholding. Figs. 5(a) and (b) displays the COM image and the resulting binary image after applying Otsu, both obtained from the original image in Fig. 1, which is a representative image from the set used for learning.

Fig. 6 displays the distribution of pixels, in the tri-dimensional RGB color space coming from the training set. Pixels labeled in green are patterns belonging to class C_1, i.e. white pixels in the corresponding binary images. On the contrary, pixels labeled as red are patterns belonging to class C_2, black pixels in the binary images. The number of pixels used for training was $800 \times 600 \times 70$. On average, the percentage of pattern samples belonging to classes C_1 and C_2 was respectively 35% and 75%. Fig. 6 also displays both kinds of support vectors surrounded by two ellipses, black points represent support vectors associated to class C_1, i.e. belonging to unmasked plants; blue points belong to masked plants.

As mentioned before, the theoretical SVM framework strictly establishes that support vectors are those associated to with the nonzero α_k, in our experiments we have discarded also α_k values where absolute values below a threshold set to 10^{-3}. On average over the total of images used for training, the number of support vectors per image was 106, with 60% and 40% associated to classes C_1 and C_2 respectively.

Table 1 displays values for the following three parameters $\boldsymbol{w}$, τ and b, computed through Eqs. (10)–(12) over the set of 7420 support vectors extracted from the set of 70 images.

From results in Table 1, two important remarks are worth emphasizing. The first is that the number of support vectors obtained by the proposed SVM, which represents only the 0.022% of the total patterns processed. The second is the very small value obtained in the margin τ; because it represents the minimal distance from the separating hyperplane from the data point, this means that data points are very close to the hyperplane and consequently classes C_1 and C_2 appear overlapped. However, the proposed strategy is able to distinguish between two types of plants, as expected.

Table 2 displays the parameter values resulting from the support vectors for classes C_1 and C_2 during the learning phase. They are averaged values for the green spectral components ($\bar{x}_u$,$\bar{x}_m$) standard deviations (σ_u, σ_m), ratios (r_{uG},r_{uG}) and tolerances (t_{uG},t_{uG}) of green.

From results in Table 2, we can see how the green spectral component in C_1 is greater than the red one. This establishes the lower limit, which is sufficient to identify unmasked plants characterized by this behavior. This does not occur in C_2, where the red spectral component is dominant, although in a small quantity; this is due to the reflectance produced for clay elements coming from the soil, which have contaminated part of the original plants. Also they can come from plants that are started the dying process because of the treatment. We can also observe the relative small difference between ratios r_{uG} and r_{mG} with the margins of tolerance expressed by t_{uG} and t_{mG}; however, the SVM framework is able to distinguish between masked, unmasked or plants affected by the treatment and also between soil pixels.

Fig. 7(a) displays the final segmented image from the original image in Fig. 2, where green and red labels inserted over the original image correspond to unmasked and masked plants respectively. We can see how most green labels are associated to crops and most red labels to weeds or crops close to the ground. In this last case, plants have been impregnated by materials coming from the soil, i.e. masking the greenness. In the first case, maize plants have not been impregnated, among other reasons because their

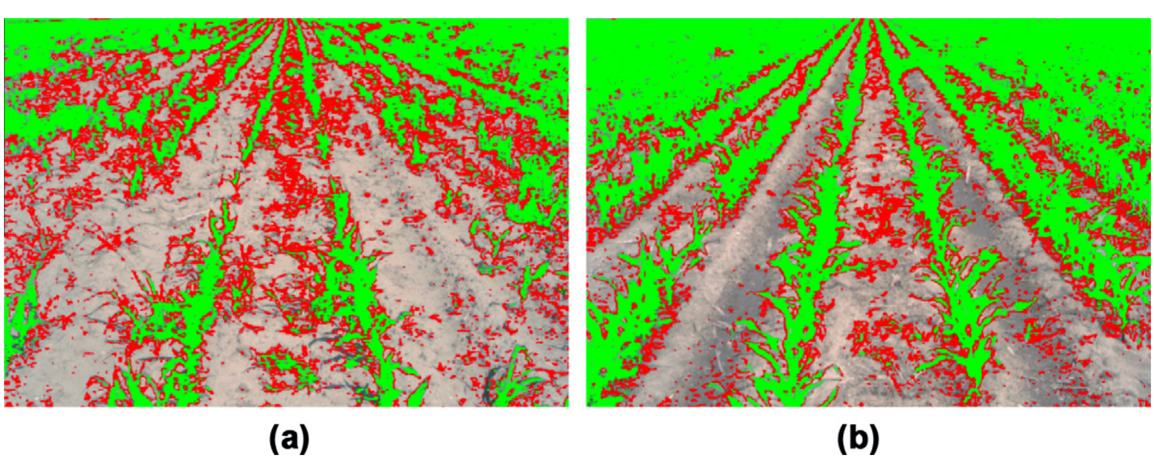

Fig. 7. Segmented images; (a) unmasked (green labels) and masked (red labels) plants from image in Fig. 2; (b) unmasked (green labels) and masked or affected by the treatment (red labels) plants from image in Fig. 3. (For interpretation of the references to colour in this figure legend, the reader is referred to the web version of this article.)

height above the ground has avoided it. This circumstance also appears for some weeds where, as before, their height avoided the impregnation.

In relation to images available for post-treatment analysis, represented by the image in Fig. 7(b), we can observe from this image how those parts close to soil appear as masked and also that an important amount of weeds on the central inter-row crops appear highly affected by the treatment having started their drying process.

Additionally, in order to assess the validity of the proposed strategy we have selected randomly 40 original images, which were visually analyzed by an expert to identify weeds plants and crops. The human visual observation is carried out for each image guided by the segmented image through the approach proposed in this paper. The expert concentrates his major effort in identifying the most troubled plants, i.e. those we call masked plants. Incorrect assignments are manually marked, corrected or removed, generating a new-segmented image, considered as the ground-truth. On average, over the set of images tested, we have obtained a percentage of success of 93.1%.

4. Conclusions

We propose a new automatic strategy for image segmentation in maize fields. The main underlying idea is the identification of support vectors, which allow to establish a region of separation between classes where masked and unmasked plants have been assigned.

The method is able to identify plants (weeds and crops) when they have been contaminated with materials coming from the soil, due to artificial irrigation or natural rainfall.

The proposed approach is also valid for monitoring the post-treatment; this is based on the assumption that weeds after chemical or mechanical treatments must initiate a progressive degradation expressed by the loss of the greenness existing in the pre-treatment stage. The damage in the crop, when it occurs, can also be analyzed based on the same criterion because of loss of greenness.

Acknowledgements

The research leading to these results has been funded by the European Union's Seventh Framework Programme [FP7/2007-2013] under Grant Agreement n° 245986 in the Theme NMP-2009-3.4-1 (Automation and robotics for sustainable crop and forestry management). The authors wish also to acknowledge to the project AGL2011-30442-C02-02, supported by the Ministerio de Economía y Competitividad of Spain within the Plan Nacional de I+D+i.

References

Burgos-Artizzu, X. P., Ribeiro, A., Guijarro, M., & Pajares, G. (2011). Real-time image processing for crop/weed discrimination in maize fields. *Computers and Electronics in Agriculture, 75*, 337–346.

Burgos-Artizzu, X. P., Ribeiro, A., Tellaeche, A., Pajares, G., & Fernández-Quintanilla, C. (2009). Improving weed pressure assessment using digital images from an experience-based reasoning approach. *Computers and Electronics in Agriculture, 65*, 176–185.

Cherkassky, V., & Mulier, F. (1998). *Learning from data: Concepts, theory and methods*. New York: Wiley.

Davies, G., Casady, W., Massey, R. (1998). Precision agriculture: An introduction. Water Quality Focus Guide (WQ450, Available on-line <http://extension.missouri.edu/explorepdf/envqual/wq0450.pdf>).

Gebhardt, S., & Kaühbauch, W. A. (2007). A new algorithm for automatic *Rumex obtusifolius* detection in digital image using colour and texture features and the influence of image resolution. *Precision Agriculture, 8*(1), 1–13.

Gebhardt, S., Schellberg, J., Lock, R., & Kaühbauch, W. A. (2006). Identification of broad-leaved dock (*Rumex obtusifolius* L.) on grassland by means of digital image processing. *Precision Agriculture, 7*(3), 165–178.

Gée, Ch., Bossu, J., Jones, G., & Truchetet, F. (2008). Crop/weed discrimination in perspective agronomic images. *Computers and Electronics in Agriculture, 60*, 49–59.

Guijarro, M., Pajares, G., Riomoros, I., Herrera, P. J., Burgos-Artizzu, X. P., & Ribeiro, A. (2011). Automatic segmentation of relevant textures in agricultural images. *Computers and Electronics in Agriculture, 75*, 75–83.

Hague, T., Tillet, N., & Wheeler, H. (2006). Automated crop and weed monitoring in widely spaced cereals. *Precision Agriculture, 1*(1), 95–113.

Kataoka, T. et al. (2003). Crop growth estimation system using machine vision. In *The 2003 IEEE/ASME internat. conf. on advanced intelligent mechatronics*.

Kirk, K., Andersen, H. J., Thomsen, A. G., & Jørgensen, J. R. (2009). Estimation of leaf area index in cereal crops using red-green images. *Biosystems Engineering, 104*, 308–317.

Ling, P. P., & Ruzhitsky, V. N. (1996). Machine vision techniques for measuring the canopy of tomato seedling. *Journal Agricultural Engineering Research, 65*(2), 85–95.

Luscier, J. D., Thompson, W. L., Wilson, J. M., Gorham, B. E., & Dragut, L. D. (2006). Using digital photographs and object-based image analysis to estimate percent ground cover in vegetation plots. *Frontiers in Ecology and the Environment, 4*(8), 408–413.

Meyer, G. E., & Camargo-Neto, J. (2008). Verification of color vegetation indices for automated crop imaging applications. *Computers and Electronics in Agriculture, 63*, 282–293.

Meyer, G. E., Camargo-Neto, J., Jones, D. D., & Hindman, T. W. (2004). Intensified fuzzy clusters for classifying plant, soil, and residue regions of interest from color images. *Computers and Electronics in Agriculture, 42*, 161–180.

Meyer, G. E., Hindman, T. W., & Lakshmi, K. (1998). *Machine vision detection parameters for plant species identification*. Bellingham, WA: SPIE.

Neto, J. C. (2004). *A combined statistical–soft computing approach for classification and mapping weed species in minimum tillage systems*. Lincoln, NE: University of Nebraska.

Onyango, C. M., & Marchant, J. A. (2003). Segmentation of row crop plants from weeds using colour and morphology. *Computers and Electronics in Agriculture, 39*, 141–155.

Otsu, N. (1979). A threshold selection method from gray-level histogram. *IEEE Transactions on Systems, Man and Cybernetics, 9*, 62–66.

Reid, J. F., & Searcy, S. W. (1987). Vision-based guidance of an agricultural tractor. *IEEE Control Systems, 7*(12), 39–43.

Ribeiro A., Fernández-Quintanilla C., Barroso J., García-Alegre, M.C. (2005). Development of an image analysis system for estimation of weed. In *Proc. 5th European conf. on, precision agriculture (5ECPA)* (pp. 169–174).

Ruiz-Ruiz, G., Gómez-Gil, J., & Navas-Gracia, L. M. (2009). Testing different color spaces based on hue for the environmentally adaptive segmentation algorithm (EASA). *Computers and Electronics in Agriculture, 68*, 88–96.

Shrestha, D. S., Steward, B. L., & Birrell, S. J. (2004). Video processing for early stage maize plant detection. *Biosystem Engineering, 89*(2), 119–129.

Tellaeche, A., Burgos-Artizzu, X. P., Pajares, G., & Ribeiro, A. (2008a). A vision-based method for weeds identification through the Bayesian decision theory. *Pattern Recognition, 41*, 521–530.

Tellaeche, A., Burgos-Artizzu, X., Pajares, G., Ribeiro, A., & Fernández-Quintanilla, C. (2008b). A new vision-based approach to differential spraying in precision agriculture. *Computers and Electronics in Agriculture, 60*(2), 144–155.

TheMathworks (2012). <http://www.mathworks.com/>.

Tian, L. F., & Slaughter, D. C. (1998). Environmentally adaptive segmentation algorithm for outdoor image segmentation. *Computers and Electronics in Agriculture, 21*, 153–168.

Vapnik, V. N. (2000). *The nature of statistical learning theory*. New York: Springer-Verlag.

Woebbecke, D. M., Meyer, G. E., von Bargen, K., & Mortensen, D. A. (1995). Shape features for identifying young weeds using image analysis. *Transactions of the American Society of Agricultural Engineering, 38*(1), 271–281.

Zheng, L., Shi, D., & Zhang, J. (2010). Segmentation of green vegetation of crop canopy images based on mean shift and Fisher linear discriminate. *Pattern Recognition Letters, 31*(9), 920–925.

Zheng, L., Zhang, J., & y Wang, Q. (2009). Mean-shift-based color segmentation of images containing green vegetation. *Computers and Electronics in Agriculture, 65*, 93–98.